AIMS Mathematics, 7(5): 8975–9002.
DOI: 10.3934/math.2022500
Received: 24 November 2021
Revised: 16 January 2022
Accepted: 27 January 2022
Published: 08 March 2022

http://www.aimspress.com/journal/Math

Research article

Influence of environmental viral load, interpersonal contact and infected rodents on Lassa fever transmission dynamics: Perspectives from fractional-order dynamic modelling

J. P. Ndenda*, J. B. H. Njagarah and S. Shaw

Department of Mathematics and Statistical Sciences, Botswana International University of Science and Technology, Private Bag 016, Palapye, Botswana

* **Correspondence:** Email: josephpn@aims.ac.za.

Abstract: Lassa fever is a fatal zoonotic hemorrhagic disease caused by Lassa virus carried by multimammate rats, which are widely spread in West Africa. In this work, a fractional-order model for Lassa fever transmission dynamics is developed and analysed. The model involves transmissions from rodents-to-human, person-to-person, as well as from Lassa virus infested environment/surfaces. The basic properties of the model such as positivity of solutions, and local stability of the disease-free equilibrium are determined. The reproduction number, $\mathcal{R}_0$, of the model is determined using the next generation method and it is used to determine the suitable conditions for disease progression as well as its containment. In addition, we performed sensitivity analysis of the model parameters using the Latin Hypercube Sampling (LHS) scheme to determine the most influential processes on the disease threshold, and determined the key processes to be focused on if the infection is to be curtailed. Moreover, fixed point theory was used to prove the existence and uniqueness of non-trivial solutions of the model. We used the Adams-Bashforth Moulton method to solve the model system numerically for different orders of the fractional derivative. Our results show that using various interventions and control measures such as controlling environmental contamination, reducing rodents-to-humans transmission and interpersonal contact, can significantly help in curbing new infections. Morestill, we observe that an increase in the memory effect, i.e. dependence on future values of the model on the previous states predicts lower peak values of infection cases in the short term, but higher equilibrium values in the long term.

Keywords: fractional-order model; Lassa virus; Mastomys rats; environmental viral load; sensitivity analysis
Mathematics Subject Classification: 92B05, 34A08, 26A33

1. Introduction

Lassa fever is a zoonotic, severe viral haemorrhage illness caused by Lassa virus, which is a member of the arenavirus family of viruses. The first cases of Lassa fever were reported in 1969 in Nigeria following the dealth of two missionary nurses. This illness is named after Lassa town in Borno State, Nigeria, where the illnesses occurred [1]. The disease is now endemic in several parts of West Africa, including Nigeria, Benin, Ghana, Mali and the Mano River region comprising of Sierra Leone, Liberia and Guinea. There is also evidence of endemicity in neighboring countries of the West African region, as the animal vector for the Lassa virus, the "multimammate rats" *(Mastomys natalensis)* species is distributed throughout the region. In some areas of Sierra Leone and Liberia, between 10% and 16% of people admitted to hospitals each year are known to have Lassa fever, indicating the serious impact of the disease in the region [2]. According to the Centers for Disease Control and Prevention (CDC), the estimated number of Lassa fever cases per year in West Africa is between 100,000 and 300,000, with about 5,000 fatalities [2, 3]. There have been some cases of Lassa fever imported into other parts of the world by travelers [4–6]. The actual incidence rate in Nigeria is unknown, but the case fatality rate ranges between 3% and 42%, (and has remained between 20% and 25% for the past two years) [1]. The disease is highly prevelent during the dry season (November to April). However, in recent years there have been outbreaks during the rainy season [1]. Various clinical conditions (such as fever, malaise, and haemorrhagic fever) accompany the disease, with people of all ages being susceptible. The onset of symptomatic disease is usually gradual, beginning with fever, general weakness, and malaise. Subsequently, headache, general weakness, malaise, sore throat, muscle pain, chest pain, nausea, vomiting, diarrhea, cough, and abdominal pain may appear. Around 80% percent of people who are infected with the Lassa virus show no symptoms. However, one-fifth of infections can cause severe illness, and the virus affects several organs including the liver, spleen, and kidneys [3]. Lassa virus infection has an overall fatality rate of 1%, but the mortality rate in hospitalized patients has been reported to be as high as 15% [3].

The animal reservoir/host for Lassa virus is a rodent of the genus Mastomys, commonly known as the "multimammate rat", which was first discovered to be infected with the virus in Nigeria and Sierra Leon in 1972, and in Guinea in 2006. Mastomys rats carry the Lassa virus but do not get sick from it. However, they can excrete the virus in urine and feces for an extended time period, maybe for the rest of their life. There is a large number of Mastomys rats living on the savannas and forests of West, Central, and Eastern Africa, and they breed frequently. Additionally, Mastomys can easily colonize human homes and food storage areas. All of these factors combined lead to a relatively efficient transmission of Lassa virus from infected Mastomys rats to humans. Humans are most commonly infected with the Lassa virus by coming into contact with the urine or faeces excreated by infected Mastomys rats. Lassa fever may also be transmitted from person to person through direct contact with blood, urine, faeces, or other bodily secretions from an infected person. Person to person transmission occurs in communities and healthcare settings, where the virus can be spread through contaminated medical equipment (such as reusable needles), eating contaminated food, and sexual transmission has been reported [3]. People living in rural areas especially in communities with poor sanitation or overcrowding are more at risk of contracting the diseases. Medical workers caring for Lassa fever patients without proper personal protective equipment, are also at risk. In the early course of the disease, the antiviral drug ribavirin may be an effective treatment. However, ribavirin lacks the evidence to support its use as a post-exposure

prophylaxis of Lassa fever [7]. There is no known vaccine that protects against Lassa fever [3].

Mathematical models have been used to analyse physical, biological, and many other complex system dynamics. Differential equation models (of discrete and continuous type) have been predominantly used in various disciplines of science to describe the dynamic features of systems. To study Lassa fever transmission dynamics, several mathematical models have been developed. Most of the models that focus on the theoretical analysis of the disease mainly consider transmission within human and Mastomys rats populations (as a reservoir). For example, in [8], the authors developed a mathematical model to explore the transmission dynamics of Lassa fever in a rodent population and the impact in human cases, while quantifying the main seasonal factors driving the infection. The authors showed that seasonal migration of rodent populations plays an important role in the seasonal transmission of the disease. Using dynamical system modelling, Ifeanyi et. al. [9] developed a multiple patch model to study the effect of socioeconomic class on Lassa fever transmission dynamics. In [9], the authors recommend that human socioeconomic classes need to be seriously considered if Lassa fever is to be completely eradicated from communities where it is endemic. A mathematical model that experiments with various control strategies in rural upper Guinea to determine the length of time and how frequently the control should be performed to eliminate Lassa fever in rural areas is presented in [10]. According to their field data analysis, it is unlikely that a yearly control strategy will reduce Lassa virus spillover to humans due to the rapid recovery of the rodent population following rodenticides application. To describe the Lassa fever risk maps in West Africa, Fichet-Calvet and Rogers [11], conducted a spatial analysis of Lassa fever data from human cases and infected rodents from 1965 to 2007. From the results of the study, it was observed that rainfall has a strong influence on defining high-risk areas, while temperature has little effect on defining high-risk areas. According to the results in the study on Lassa fever infection with control in two different but complementary hosts [12], the best way to control secondary transmission dynamics from human-to-human is to establish more Lassa fever diagnostic centers and use precautionary burial practices. In addition, the study by Ojo et. al [13], indicates that any control strategies and methods that reduce rodent populations and the risk of transmission from rodents to humans would aid in the control the disease.

In the aforementioned articles, no study considered the contribution of environmental contamination to the dynamics of the Lassa virus. In addition, the mathematical models considered do not sufficiently account for the memory as well as nonlocal properties that may be exhibited by the epidemic system under consideration owing to the evolutionary trends and dependence of future numbers of cases on previous states. Employing fractional calculus in the Lassa fever model considered in this paper provides an appropriate tool to account for the nonlocal behavior and memory of the proposed epidemic system. As indicated in [14], reducing the order of the fractional derivative from 1 toward 0 accounts for the increase in memory effect in the dynamical system considered. Therefore, owing to the evolutionary trends associated with resistance to virulence, the nonlocal assumption, and the memory effect with respect to time, it is justified to use fractional-order derivatives to study the trends of Lassa fever in a human population.

The theory of Fractional calculus has been employed in studying the dynamics of real-world problems in various areas which include but not limited to physics, fluid mechanics, finance, and mathematical biology, see [15–21]. Recently, several approaches have been used for the generalization of fractional order differentiation [22–27], the Riemann-Liouville [23, 27, 28], Liouville–Caputo-fractional derivative [22, 23, 29], Caputo-Fabrizio fractional derivative [23, 30], and Atangana-Baleanu

function approaches [23, 31], among others. Since the Caputo derivative has flexibility with handling initial value problems [22, 23], we use the Caputo-Fabrizio (CF) fractional derivative to model the dynamics of Lassa fever. The CF fractional derivative has also been used recently to study several epidemic models including hepatitis B virus [32], malaria transmission dynamics [33], modeling chickenpox disease, pine wilt disease, smoking dynamics, metapopulation cholera transmission dynamics, tumor-immune system [16, 34, 35], and Covid-19 transmission dynamics [36–42] among others.

The rest of the manuscript is organized as follows: The model formulation, analysis of the basic properties including the region of biological significance, reproduction number, stability, and the existence and uniqueness of solutions using the fixed point theory are presented in Section 2. In Section 3, numerical simulations and results are presented. The conclusion of the manuscript and future work are presented in Section 4.

2. Mathematical model formulation and analysis

In this section, we give a description of a mathematical model for Lassa fever that considers the human population, mastomys rats population together with contaminated surfaces or objects in the environment. We assume that the populations have homogeneous spatial distribution as well as mixing within subpopulations. The human population is divided into susceptible (S), exposed (E), asymptomatic infected (A), symptomatic infected (I), hospitalized (H), and recovered (R) categories, so that the total human population $N(t)$ at any time t is given by

$$N(t) = S(t) + E(t) + A(t) + I(t) + H(t) + R(t).$$

The mastomys rats population is divided into susceptible mastomys rats (S_r) and infected mastomys rats (I_r) categories. We note that infected mastomys rates carry the Lassa fever causing pathogen but are not affected by the pathogen. Thus, the total mastomys rats population, $N_r(t)$ is given by

$$N_r(t) = S_r(t) + I_r(t).$$

In this model, the contribution of the environment to the spread of Lassa virus is included in such a way that V represents the Lassa virus pathogens concentration contaminating the surfaces or objects in the environment due to shedding of the virus from infected individuals or mastomys rats. The formulation of the model is based on the following cosiderations:

- Mastomys rats shed the virus through urine or faeces and direct contact with virus infested materials, through touching of soiled household objects, eating contaminated food, or exposure to open wounds or sores, can lead to infection [1–3].
- Contact with the virus may also occur when a person inhales tiny particles in the air contaminated with infected mastomys rats excrements. Usually, this aerosol or airborne transmission may occur during cleaning activities, such as floor sweeping [2].
- Mastomys rats are sometimes consumed as a source of food in some communities and infection may occur during rodents capture and grooming [2].
- In addion, person-to-person transmission may occur particularly in healthcare settings, in the absence of proper personal protective equipment (PPE), or when PPEs are not used [1–3].

- Infected mastomys rats can excrete the virus in urine for an extended period, and possibly for the rest of their lives [2].

Combining the above considerations, the force infection (λ) for the human population, is given by

$$\lambda = \beta_1 \left(\frac{I + \eta_1 A + \eta_2 H}{N} \right) + \beta_2 \left(\frac{I_r}{N_r} \right) + \beta_3 \left(\frac{V}{\kappa + V} \right),$$

where β_1 and β_2 are the human-to-human contact rate and mastomys rat-to-human contact rate, respectively. In addition, the human exposure rate β_3 to free viruses in contaminated environments is assumed to follow a logistic-dose response curve or Hill function $\frac{V}{\kappa+V}$, where κ is the concentration of the Lassa virus in the environment which increases the chance of triggering the disease transmission by 50%. The parameters η_1, and η_2 are transmissibility multiple that measure the transmission rates due to contact with asymptomatic infected individuals (A), and hospitalized individuals (H) relative to the transmission rate due to symptomatically infected individuals, respectively. The force of infection of mastomys rats (λ_r) is given by

$$\lambda_r = \beta_4 \left(\frac{I_r}{N_r} \right) + \beta_5 \left(\frac{V}{\kappa + V} \right),$$

where β_4 is mastomys rat-to-mastomys rat contact rate, and β_5 is the mastomys rats exposure rate to free viruses in the environment. Figure 1 shows a schematic representation of the mathematical model for Lassa fever transmission. Tables 1 and 2 show a detailed descriptions of the state variables and the model parameters, respectively.

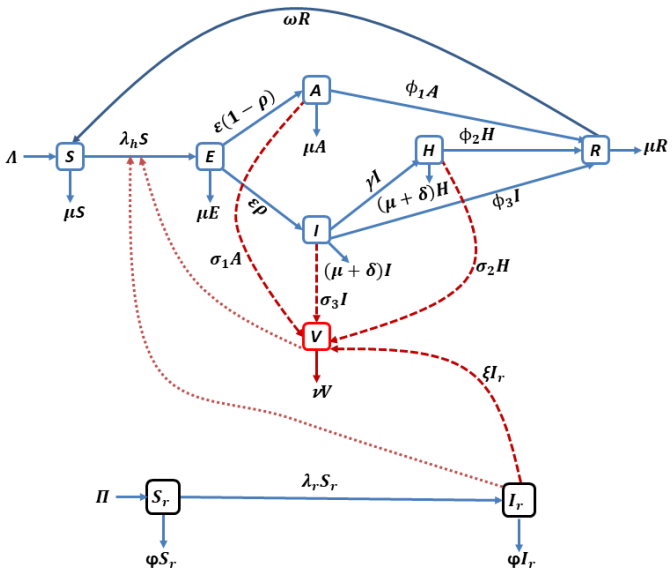

Figure 1. Schematic diagram of Lassa fever transmission dynamics describing the interaction between human and the mastomys rats population, as well as a virus infested environment.

Table 1. Description of the model state variables.

Variable	Description
S	Susceptible individuals
E	Exposed individuals
A	Asymptomatic infected individuals
I	Symptomatic infected individuals
H	Hospitalized individuals
R	Recovered individuals
V	Contaminated surfaces or objects in the environment.
S_r	Susceptible mastomys rats
I_r	Infected mastomys rats

Table 2. Description of the model variables.

Parameters	Description
Λ	Rate of recruitment into the susceptible population
μ	Natural mortality rate of the human population
ρ	Proportion of new exposed individual that become symptomatically infected
ϵ	Rate at which an exposed individual becomes infectious
γ	Rate at which symptomatic individual require hospitalization
ϕ_1, ϕ_3, ϕ_2	Recovery rate for the asymptomatic, symptomatic and hospitalized individuals
δ	Disease-induced death rate
ω	Rate at which immunity wanes after recovery
σ_1	Rate at which the asymptomatic infected shed the virus into the environment
σ_2	Rate at which hospitalized patients shed the virus into the environment
σ_3	Rate at which symptomatic patients shed the virus into the environment
ξ	Rate at which infected mastomys rat shed virus into the environment
ν	Virus decay rate from the environment (Surfaces)
Π	Recruitment (birth) rate into mastomys rats population
φ	Natural mortality rate of mastomys rats
β_1	Human-to-human contact rate
β_2	Mastomys rats-to-human contact rate
β_3	Rate of human contact with infected surfaces/environment
β_4	Mastomys rat-to-mastomys rat contact rate
β_5	Rate of Mastomys rat contact with infected surfaces in the environment
κ	Concentration of Lassa virus in the environment
η_1	Transmission rate of infective individuals in A relative to those in I
η_2	Transmission rate of infective individuals in H relative to those in I

Following the discussion above, we formulate the system of fractional order differential equations for Lassa fever dynamics as

$$\begin{cases} {}^{C}D^{\alpha}S = \Lambda - \lambda S + \omega R - \mu S \\ {}^{C}D^{\alpha}E = \lambda S - Q_1 E \\ {}^{C}D^{\alpha}A = \varepsilon(1-\rho)E - Q_2 A \\ {}^{C}D^{\alpha}I = \varepsilon\rho E - Q_3 I \\ {}^{C}D^{\alpha}H = \gamma I - Q_4 H \\ {}^{C}D^{\alpha}R = \phi_1 A + \phi_2 H + \phi_3 I - Q_5 R \\ {}^{C}D^{\alpha}V = \sigma_1 A + \sigma_2 H + \sigma_3 I + \xi I_r - \nu V \\ {}^{C}D^{\alpha}S_r = \Pi - \lambda_r S_r - \varphi S_r, \\ {}^{C}D^{\alpha}I_r = \lambda_r S_r - \varphi I_r, \end{cases} \tag{2.1}$$

where ${}^{C}D^{\alpha}$ represents the Caputo-Fabrizio fractional derivative of order $0 < \alpha \leq 1$, with

$$\begin{cases} Q_1 = \varepsilon + \mu, \quad Q_2 = \phi_1 + \mu, \quad Q_3 = \phi_3 + \gamma + \delta + \mu, \\ Q_4 = \phi_2 + \delta + \mu, \quad Q_5 = \omega + \mu, \end{cases}$$

and the corresponding nonnegative initial conditions are such that

$$\begin{cases} S(0) > 0, E(0) > 0, A(0) > 0, H(0) > 0, I(0) > 0, R(0) > 0, \\ V(0) > 0, S_r(0) > 0, \text{ and } I_r(0) > 0. \end{cases} \tag{2.2}$$

2.1. Boundedness and positivity

In this section, we prove the positivity and boundedness of the solutions to ensure that the system of equations (2.1), is mathematically well defined and biologically meaningful.

Theorem 1. *Given the positive initial conditions* (2.2)*, the solutions of the model system* (2.1) *are all non-negative for* $t > 0$*.*

Proof. To prove the non-negativity of the solutions of the fractional-order system (2.1), we consider the resulting eqution for each of the state variables such that

$$\begin{aligned} {}^{C}D^{\alpha}S|_{S=0} &= \Lambda + \omega R \geq 0, \\ {}^{C}D^{\alpha}E|_{E=0} &= \lambda S \geq 0, \\ {}^{C}D^{\alpha}A|_{A=0} &= \epsilon(1-\rho)E \geq 0, \\ {}^{C}D^{\alpha}I|_{I=0} &= \epsilon\rho E \geq 0, \\ {}^{C}D^{\alpha}H|_{H=0} &= \gamma I \geq 0, \\ {}^{C}D^{\alpha}R|_{R=0} &= \phi_1 A + \phi_2 H + \phi_3 I \geq 0, \\ {}^{C}D^{\alpha}V|_{V=0} &= \sigma_1 A + \sigma_2 H + \sigma_3 I + \xi I_r \geq 0, \\ {}^{C}_{0}D^{\alpha}I_v|_{I_v=0} &= \lambda_r S_r \geq 0. \end{aligned} \tag{2.3}$$

Following the approach detailed in Lemma 1 and Remark 1 in [16], as well as the reduced system (2.3), one can deduce that the solutions of the fractional-order system (2.1) are non-negative for all $t \geq 0$. □

Theorem 2. *The invariant region* Ω *for the model* (2.1) *with initial conditions* (2.2) *defined by*

$$\Omega = \Omega_p \times \Omega_v \times \Omega_r,$$

where

$$\Omega_p = \left\{(S, E, A, I, H, R) \in \mathbb{R}_+^6\right\}, \quad \Omega_v = \left\{(V) \in \mathbb{R}_+^1\right\}, \quad \Omega_r = \left\{(S_r, I_r) \in \mathbb{R}_+^2\right\},$$

such that

$$\left\{0 \leq N(t) \leq \frac{\Lambda}{\mu}, \quad 0 \leq V(t) \leq \left((\sigma_1 + \sigma_2 + \sigma_3)\left(\frac{\Lambda}{\mu}\right) + \xi\left(\frac{\Pi}{\varphi}\right)\right)\frac{1}{\nu}, \;\; 0 \leq N_r(t) \leq \frac{\Pi}{\varphi}\right\},$$

is positively invariant for all $t \geq 0$.

Proof. By considering the system of equations (2.1), the change in the total human population at any given time is given by

$$\begin{aligned} {}_0^C D^\alpha N &= \Lambda - \mu N - \delta I - \delta H, \\ {}_0^C D^\alpha N &\leq \Lambda - \mu N. \end{aligned} \tag{2.4}$$

Then, the inequality (2.4) can be written as a Cauchy problem such that

$${}_0^C D^\alpha N \leq \Lambda - \mu N, \quad N(0) = N_0 \in \mathbb{R},$$

whose solution is given in terms of a Mittag-Leffler function [23] as

$$N(t) \leq N_0 E_\alpha[-\mu t^\alpha] + \Lambda \int_0^t (t-s)^{\alpha-1} E_{\alpha,\alpha}[-\mu(t-s)^\alpha] ds. \tag{2.5}$$

Since from [43],

$$\int_0^t (t-s)^{\alpha-1} E_{\alpha,\alpha}[-\mu(t-s)^\alpha] ds = t^\alpha E_{\alpha,\alpha+1}[-\mu t^\alpha],$$

then, the solution (2.5) can be written as

$$N(t) \leq N_0 E_\alpha[-\mu t^\alpha] + \Lambda t^\alpha E_{\alpha,\alpha+1}[-\mu t^\alpha].$$

We observe that as $t \longrightarrow \infty$, then $E_\alpha[-\mu t^\alpha] \longrightarrow 0$, and $E_{\alpha,\alpha+1}[-\mu t^\alpha] \longrightarrow \frac{1}{\mu}$ [44], which results in

$$N(t) \leq \frac{\Lambda}{\mu}. \tag{2.6}$$

Similarly, for the total mastomys rats population, we have a Cauchy problem given by

$${}_0^C D^\alpha N_r = \Pi - \varphi N_r, \quad N_r(0) = N_{r_0} \in \mathbb{R},$$

whose solution is given by

$$N_r(t) \leq N_{r_0} E_\alpha[-\varphi t^\alpha] + \Pi \int_0^t (t-s)^{\alpha-1} E_{\alpha,\alpha}[-\varphi(t-s)^\alpha] ds,$$

such that

$$N_r(t) = \frac{\Pi}{\varphi}. \tag{2.7}$$

For the concentration of virus in the environment, we have

$$_0^C D^\alpha V = \sigma_1 A + \sigma_2 H + \sigma_3 I + \xi I_r - \nu V,$$

which can be written as a Cauchy problem

$$_0^C D^\alpha V \leq (\sigma_1 + \sigma_2 + \sigma_3)\left(\frac{\Lambda}{\mu}\right) + \xi\left(\frac{\Pi}{\varphi}\right) - \nu V, \quad V(0) = V_0 \in \mathbb{R}, \tag{2.8}$$

since $0 < (A + H + I) \leq \frac{\Lambda}{\mu}$ and $0 < I_r \leq \frac{\Pi}{\varphi}$ for all $t \leq 0$.
The solution of the Cauchy problem (2.8) is given in terms of a Mittag-Leffler function as

$$V(t) \leq V_0 E_\alpha[-\nu t^\alpha] + \left((\sigma_1 + \sigma_2 + \sigma_3)\left(\frac{\Lambda}{\mu}\right) + \xi\left(\frac{\Pi}{\varphi}\right)\right)\int_0^t (t-s)^{\alpha-1} E_{\alpha,\alpha}[-\nu(t-s)^\alpha]ds.$$

We note that as $t \longrightarrow \infty$, the solution simplifies to

$$V(t) \leq \left((\sigma_1 + \sigma_2 + \sigma_3)\left(\frac{\Lambda}{\mu}\right) + \xi\left(\frac{\Pi}{\varphi}\right)\right)\frac{1}{\nu}. \tag{2.9}$$

This indicates that none of the state variables grows without bound. □

Owing to the results of positivity and boundeness of solutions, the model system (2.1) is well posed and positively invariant in the domain Ω. Therefore, it is feasible to analyse the dynamics of the system (2.1) in domain Ω.

2.2. Disease free equilibrium and basic reproduction number

To determine the disease-free equilibrium of model system (2.1), we assume there is no Lassa fever by letting $E = A = I = H = R = V = I_r = 0$. Then, the system of equations (2.1) reduces to

$$\begin{cases} _0^C D^\alpha S = \Lambda - \mu S, \\ _0^C D^\alpha S_r = \Pi - \varphi S_r. \end{cases} \tag{2.10}$$

Therefore, solving the stationary points of the resulting system with (2.10), yields

$$\mathcal{E}_0 = \left(\frac{\Lambda}{\mu}, 0, 0, 0, 0, 0, 0, \frac{\Pi}{\varphi}, 0\right),$$

which is the disease-free equilibrium. The basic reproduction number $\mathcal{R}_0$ is very important for the qualitative analysis of the model, as it indicates the average number of new Lassa fever infections that will be generated in a wholly susceptible human population when an infected individual or rat is introduced. To obtain the basic reproduction number $\mathcal{R}_0$, we consider the case when $\alpha = 1$, and follow the next-generation method detailed in [45]. By considering the infected compartments $\mathcal{X} =$

(E, A, I, H, V, I_r) the Jacobian matrices F for the new infection terms, and V_e for the remaining transfer terms evaluated at the disease free equilibrium are respectively given by

$$F = \begin{pmatrix} 0 & \beta_1\eta_1 & \beta_1 & \beta_1\eta_2 & \frac{\beta_3\Lambda}{\kappa_1\mu} & \frac{\beta_2\Lambda\varphi}{\mu\Pi} \\ 0 & 0 & 0 & 0 & 0 & 0 \\ 0 & 0 & 0 & 0 & 0 & 0 \\ 0 & 0 & 0 & 0 & 0 & 0 \\ 0 & 0 & 0 & 0 & 0 & 0 \\ 0 & 0 & 0 & 0 & \frac{\beta_5\Pi}{\kappa_2\varphi} & \beta_4 \end{pmatrix},$$

and

$$V_e = \begin{pmatrix} Q_1 & 0 & 0 & 0 & 0 & 0 \\ -\varepsilon(1-\rho) & Q_2 & 0 & 0 & 0 & 0 \\ -\varepsilon\rho & 0 & Q_3 & 0 & 0 & 0 \\ 0 & 0 & -\gamma & Q_4 & 0 & 0 \\ 0 & -\sigma_1 & -\sigma_3 & -\sigma_2 & \nu & -\xi \\ 0 & 0 & 0 & 0 & 0 & \varphi \end{pmatrix}.$$

Then the basic reproduction $\mathcal{R}_0$ of the model system (2.1) is the spectral radius of the next-generation FV_e^{-1}, such that

$$\mathcal{R}_0 = \frac{\mathcal{R}_0^{hhv} + \mathcal{R}_0^{rrv} + \sqrt{\left(\mathcal{R}_0^{hhv} - \mathcal{R}_0^{rrv}\right)^2 + 4\mathcal{R}_0^{hrv}\mathcal{R}_0^{rhv}}}{2},$$

where the term

$$\mathcal{R}_0^{hhv} = \mathcal{R}_0^{hh} + \mathcal{R}_0^{hv},$$

such that

$$\begin{aligned}
\mathcal{R}_0^{hh} &= \frac{\beta_1\eta_1 Q_3Q_4\kappa_1\nu\mu\epsilon(1-\rho) + \beta_1\eta_2 Q_2\gamma\kappa_1\nu\mu\rho\epsilon + \beta_1\epsilon\rho\kappa_1\nu\mu Q_2Q_4}{Q_1Q_2Q_3Q_4\kappa_1\mu\nu}, \\
\mathcal{R}_0^{hv} &= \frac{\Lambda Q_2Q_4\beta_3\epsilon\rho\sigma_3 + \Lambda Q_2\beta_3\epsilon\gamma\rho\sigma_2 + \Lambda Q_3Q_4\beta_3\epsilon\sigma_1(1-\rho)}{Q_1Q_2Q_3Q_4\kappa_1\mu\nu}, \\
\mathcal{R}_0^{rrv} &= \frac{\beta_4\kappa_2\nu\varphi + \Pi\beta_5\xi}{\kappa_2\nu\varphi^2}, \\
\mathcal{R}_0^{hrv} &= \frac{\Lambda\beta_2\kappa_1\nu\varphi + \Lambda\Pi\beta_3\xi}{\Pi\kappa_1\mu\nu\varphi}, \\
\mathcal{R}_0^{rhv} &= \frac{\Pi Q_2\beta_5\epsilon\gamma\sigma_2\rho + \Pi Q_2Q_4\beta_5\epsilon\rho\sigma_3 + \Pi Q_3Q_4\beta_5\sigma_1\epsilon(1-\rho)}{Q_1Q_2Q_3Q_4\kappa_2\nu\varphi}.
\end{aligned}$$

The term $\mathcal{R}_0^{hh}$ is the contribution of human-to-human contact, and $\mathcal{R}_0^{hv}$ indicates the contribution of human contact with the virus shed into the environment by infected humans. The term $\mathcal{R}_0^{rrv}$ indicates the number of new infected rats resulted from rat-to-rat contact, and rat contact with the virus shed into the environment by infected rats. The term $\mathcal{R}_0^{hrv}$ indicates the number of new infected humans generated from direct contact with infected rat, and the virus shed into the environment by infected rats. The term $\mathcal{R}_0^{rhv}$ indicates the number of new infected rats generated from contact with the virus shed by infected humans into the environment. A square root in the reproduction number in the view

that the disease transmission takes two generations. According to [45], computation of $\mathcal{R}_0$ using the next-generation method presumes locally stability of the disease free equilibrium. Therefore we have the following Theorem.

Theorem 3. *The disease-free equilibrium of model* (2.1) *is locally asymptotically stable whenever* $\mathcal{R}_0 < 1$ *and unstable if* $\mathcal{R}_0 > 1$.

The epidemiological implication of Theorem 3 is that the transmission of Lassa fever can be controlled by enhancing or containing the processes that can result in reducing $\mathcal{R}_0$ to value below 1.

2.3. Existence and uniqueness of a system of solutions

Here, we examine the existence and uniquenence of the model system solution. The Fixed Point Theory is applied to study the existence of the solutions of the model system (2.1). We use the summarised procedure in [18] to rewrite model system (2.1) in the form

$$ {}_0^C D^{\alpha} y(t) = f(t, y(t)), \quad y(0) = y_0, \tag{2.11} $$

where

$$ y(t) = \{S(t), E(t), A(t), I(t), H(t), R(t), V(t), S_r(t), I_r(t)\}, $$

such that

$$ f(t, y(t)) = \begin{pmatrix} f^1(t, y^1(t)) \\ f^2(t, y^2(t)) \\ f^3(t, y^3(t)) \\ f^4(t, y^4(t)) \\ f^5(t, y^5(t)) \\ f^6(t, y^6(t)) \\ f^7(t, y^7(t)) \\ f^8(t, y^8(t)) \\ f^9(t, y^9(t)) \end{pmatrix} = \begin{pmatrix} \Lambda + \omega R(t) - \lambda S(t) - \mu S(t) \\ \lambda S(t) - Q_1 E(t) \\ \varepsilon(1-\rho)E(t) - Q_2 A(t) \\ \varepsilon\rho E(t) - Q_3 I(t) \\ \gamma I(t) - Q_4 H(t) \\ \phi_1 A(t) + \phi_2 H(t) + \phi_3 I(t) - Q_5 R(t) \\ \sigma_1 A(t) + \sigma_2 H(t) + \sigma_3 I(t) + \xi I_r(t) - \nu V(t) \\ \Pi - \lambda_r S_r(t) - \varphi S_r(t) \\ \lambda_r S_r(t) - \varphi I_r(t) \end{pmatrix}, $$

with

$$ y(0) = \{S(0), E(0), A(0), I(0), H(0), R(0), V(0), S_r(0), I_r(0)\}. $$

Using the fractional integral operator proposed by Losada and Nieto [46] on (2.11), we have

$$ y^i(t) - y^i(0) = {}_0^{CF} I_t^{\alpha} f^i(t, y^i(t)), \text{ for } i = 1, 2, \ldots, 9. \tag{2.12} $$

Following the notation used in [46], the equations in (2.12) yield

$$ y^i(t) - y^i(0) = \frac{2(1-\alpha)}{(2-\alpha)M(\alpha)} \{f^i(t, y^i(t))\} + \frac{2\alpha}{(2-\alpha)M(\alpha)} \int_0^t \left\{f^i(x, y^i(x))\right\} dx. \tag{2.13} $$

For simplicity, the system (2.13) can be written as

$$ K_i(t, y^i) = f^i(t, y^i(t)), \text{ for } i = 1, 2, \ldots, 9. \tag{2.14} $$

Theorem 4. *The kernels K_i satisfy the Lipschitz conditions and contraction, if the inequalities*

$$\|K_i(t, y^i) - K_i(t, y^{i*})\| \leq \psi_i \|y^i(t) - y^{i*}\| \quad \textit{and} \quad 0 \leq \psi_i < 1$$

hold for $i = 1, 2, 3, \ldots 9$, where

$$\psi_1 = (\lambda^* + \mu), \quad \psi_2 = Q_1, \quad \psi_3 = Q_2, \quad \psi_4 = Q_3, \quad \psi_5 = Q_4,$$
$$\psi_6 = Q_5, \quad , \psi_7 = \nu, \quad , \psi_8 = (b + \varphi), \quad \textit{and} \quad \psi_9 = \varphi.$$

Proof. First, we start with kernel K_1. Considering $y^1(t) = S(t)$ and $y^{1*}(t) = S^*(t)$ as two functions, we have

$$\|K_1(t, y^1) - K_1(t, y^{1*})\| = \| - \lambda \left(y^1(t) - y^{1*}(t)\right) - \mu \left(y^1(t) - y^{1*}(t)\right) \|.$$

By using the triangle inequality, we get

$$\|K_1(t, y^1) - K_1(t, y^{1*})\| \leq \|\lambda \left(y^1(t) - y^{1*}(t)\right) \| + \|\mu \left(y^1(t) - y^{1*}(t)\right) \|$$
$$\|K_1(t, y^1) - K_1(t, y^{1*})\| \leq (\lambda^* + \mu) \|y^1(t) - y^{1*}(t)\|,$$

considering that

$$\psi_1 = (\lambda^* + \mu),$$

where $\lambda^* = \max_{t \geq 0} \|\lambda(t)\|$ is a bounded function, we have

$$\|K_1(t, y^1) - K_1(t, y^{1*})\| \leq \psi_1 \|y^1(t) - y^{1*}(t)\|.$$

Hence, the kernel K_1 satisfies the Lipschitz condition and the contraction when $0 \leq \psi_1 < 1$. In a similar way, the remaining kernels meet the criterior for Lipschitz condition, and can be expressed as follows:

$$\|K_i(t, y^i) - K_i(t, y^{i*})\| \leq \psi_i \| \left(y^i(t) - y^{i*}(t)\right) \|, \text{ for } i = 2, 3, \ldots, 9.$$

Taking into account the kernels (2.14), the system of equations (2.13) becomes

$$y^i(t) = y^i(0) + \frac{2(1-\alpha)}{(2-\alpha)M(\alpha)} K_i(t, y^i) + \frac{2\alpha}{(2-\alpha)M(\alpha)} \int_0^t K_i(x, y^i) dx. \tag{2.15}$$

Then, we define the following recursive formulas

$$y^i_n(t) = \frac{2(1-\alpha)}{(2-\alpha)M(\alpha)} K_i(t, y^i_{n-1}) + \frac{2\alpha}{(2-\alpha)M(\alpha)} \int_0^t K_i(x, y^i_{n-1}) dx, \tag{2.16}$$

with initial conditions

$$y^i_0(t) = y^i(0).$$

In these cases, we present the differences between the successive terms as:

$$\Psi_{i_n} = y^i_n(t) - y^i_{n-1}(t) = \frac{2(1-\alpha)}{(2-\alpha)M(\alpha)} \left[K_i(t, y^i_{n-1}) - K_i(t, y^i_{n-2})\right]$$

$$+\frac{2\alpha}{(2-\alpha)M(\alpha)}\int_0^t [K_i(x,y^i_{n-1})-K_i(x,y^i_{n-2})]dx. \tag{2.17}$$

It is essential to note that

$$y^i_n(t)=\sum_{j=0}^{n}\Psi_{i_j}. \tag{2.18}$$

By following a step by step approach, we get

$$\begin{aligned}\|\Psi_{i_n}\| &= \|y^i_n(t)-y^i_{n-1}(t)\|\\ &= \left\|\frac{2(1-\alpha)}{(2-\alpha)M(\alpha)}[K_i(t,y^i_{n-1})-K_i(t,y^i_{n-2})]\right.\\ &\quad \left.+\frac{2\alpha}{(2-\alpha)M(\alpha)}\int_0^t [K_i(x,y^i_{n-1})-K_i(x,y^i_{n-2})]dx\right\|.\end{aligned} \tag{2.19}$$

Applying triangle inequality, equation (2.19) reduces to:

$$\begin{aligned}\|\Psi_{i_n}\| &\le \frac{2(1-\alpha)}{(2-\alpha)M(\alpha)}\left\|[K_i(t,y^i_{n-1})-K_i(t,y^i_{n-2})]\right\|\\ &\quad +\frac{2\alpha}{(2-\alpha)M(\alpha)}\left\|\int_0^t [K_i(x,y^i_{n-1})-K_i(x,y^i_{n-2})]dx\right\|\end{aligned} \tag{2.20}$$

Considering the fact that the kernels satisfy the Lipschitz condition, we obtain:

$$\begin{aligned}\|\Psi_{i_n}\| &\le \frac{2(1-\alpha)}{(2-\alpha)M(\alpha)}\psi_i\left\|y^i_{n-1}-y^i_{n-2}\right\|+\frac{2\alpha}{(2-\alpha)M(\alpha)}\int_0^t \psi_i\left\|y^i_{n-1}-y^i_{n-2}\right\|dx,\\ &\le \frac{2(1-\alpha)}{(2-\alpha)M(\alpha)}\psi_i\left\|\Psi_{1_{n-1}}(t)\right\|+\frac{2\alpha}{(2-\alpha)M(\alpha)}\int_0^t \psi_i\left\|\Psi_{i_{n-1}}(t)\right\|dx,\ \text{for } i=1,2,3,\ldots,9.\end{aligned} \tag{2.21}$$

□

Theorem 5. *The fractional-order model* (2.1)*, has a solution if there exists* t_0 *such that [46]*

$$\frac{2(1-\alpha)}{(2-\alpha)M(\alpha)}\psi_i+\frac{2\alpha}{(2-\alpha)M(\alpha)}\psi_i t_0\le 1,\quad i\in\{1,2,\ldots,9\}.$$

Proof. We consider that the functions $y^i(t)$ are bounded, and kernel fulfills the Lipschitz condition. From the results of Eq (2.21), we utilize a recursive techniques to obtain the relations

$$\|\Psi_{i_n}\|\le\|y^i(0)\|\left[\frac{2(1-\alpha)}{(2-\alpha)M(\alpha)}\psi_i+\frac{2\alpha}{(2-\alpha)M(\alpha)}\psi_i t_0\right]^n. \tag{2.22}$$

Now, we need to show that the functions in (2.22) are the system of solutions associated with the model system (2.1). We suppose that

$$y^i(t)-y^i(0)=y^i_n(t)-w^i_n(t).$$

Then

$$\begin{aligned}\|w_n^i(t)\| &= \left\| \frac{2(1-\alpha)}{(2-\alpha)M(\alpha)}[K_i(t,y_n^i) - K_i(t,y_{n-1}^i)] + \frac{2\alpha}{(2-\alpha)M(\alpha)}\int_0^t [K_i(x,y_n^i) - K_i(x,y_{n-1}^i)]dx \right\|, \\ &\leq \frac{2(1-\alpha)}{(2-\alpha)M(\alpha)}\left\|[K_i(t,y_n^i) - K_i(t,y_{n-1}^i)]\right\| + \frac{2\alpha}{(2-\alpha)M(\alpha)}\int_0^t \left\|[K_i(x,y_n^i) - K_i(x,y_{n-1}^i)]\right\| dx, \\ &\leq \frac{2(1-\alpha)}{(2-\alpha)M(\alpha)}\psi_1\left\|y_n^i - y_{n-1}^i\right\| + \frac{2\alpha}{(2-\alpha)M(\alpha)}\psi_1\left\|y_n^i - y_{n-1}^i\right\| t.\end{aligned}$$

By employing the recursive technique, we obtain

$$\|w_n^i(t)\| \leq \left(\frac{2(1-\alpha)}{(2-\alpha)M(\alpha)} + \frac{2\alpha}{(2-\alpha)M(\alpha)}t\right)^{n-1}\psi_i^{n-1}\nu. \tag{2.23}$$

Taking the limit on the Eq (2.23) as n tends to infinity, yields

$$\|w_n^i(t)\| \longrightarrow 0.$$

Hence, existence of solutions is satisfied. □

Theorem 6. *The system of Eq* (2.1) *has a unique solution if the condition [46]*

$$\left(1 - \frac{2(1-\alpha)}{(2-\alpha)M(\alpha)}\psi_i - \frac{2\alpha}{(2-\alpha)M(\alpha)}\psi_i t\right) \geq 0 \tag{2.24}$$

is satisfied.

Proof. We assume that there exists another system of solutions of the model (2.1), such as y_1^i. Then,

$$\begin{aligned}y^i(t) - y_1^i(t) &= \frac{2(1-\alpha)}{(2-\alpha)M(\alpha)}[K_i(t,y^i) - K_i(t,y_1^i)] \\ &\quad + \frac{2\alpha}{(2-\alpha)M(\alpha)}\int_0^t [K_i(x,y^i) - K_i(x,y_1^i)]dx.\end{aligned} \tag{2.25}$$

Applying the norm on both sides of Eq (2.25) yields

$$\begin{aligned}\|y^i(t) - y_1^i(t)\| &\leq \frac{2(1-\alpha)}{(2-\alpha)M(\alpha)}\|[K_i(t,y^i) - K_i(t,y_1^i)]\| \\ &\quad + \frac{2\alpha}{(2-\alpha)M(\alpha)}\int_0^t \|[K_i(x,y^i) - K_i(x,y_1^i)]\|dx.\end{aligned} \tag{2.26}$$

By using the Lipschitz condition of the kernels, we have

$$\|y^i(t) - y_1^i(t)\| \leq \frac{2(1-\alpha)}{(2-\alpha)M(\alpha)}\psi_i\|y^i(t) - y_1^i(t)\| + \frac{2\alpha}{(2-\alpha)M(\alpha)}\|y^i(t) - y_1^i(t)\|\psi_i t \tag{2.27}$$

Thus, it becomes

$$\|y^i(t) - y_1^i(t)\|\left(1 - \frac{2(1-\alpha)}{(2-\alpha)M(\alpha)}\psi_1 - \frac{2\alpha}{(2-\alpha)M(\alpha)}\psi_1 t\right) \leq 0 \tag{2.28}$$

If the condition (2.24) exists, then Eq (2.28) satisfies the equality and thus

$$\|y^i(t) - y_1^i(t)\| = 0,$$

which implies that

$$y^i(t) = y_1^i(t).$$

This proves the uniqueness of the solutions of the model system (2.1). □

3. Numerical simulations

Several numerical techniques have been proposed to solve fractional-order differential equations, such as the Adomian Decomposition Method, the Homotopy Decomposition Method, the Adams-Bashforth-Moulton Method among others. Here, we use the Adams-Bashforth-Moulton method to provide an approximate solution for the dynamic model based on the Predator-Corrector algorithm. We set $h = \frac{T}{N}$, $t_n = nh$ and $n = 0, 1, 2, \ldots N \in \mathbb{Z}^+$ [47, 48]. Then model system (2.1) can be discretized following the approach in [18, 19].

The corrector values

$$
\begin{aligned}
S_{n+1} &= S_0 + \frac{h^\alpha}{\Gamma(\alpha+2)}\left[\Lambda - \left(\beta_1\frac{I^p_{n+1} + \eta_1 A^p_{n+1} + \eta_2 H^p_{n+1}}{N^p_{n+1}} + \beta_2\frac{I^p_{r_{n+1}}}{N^p_{r_{n+1}}} + \beta_3\frac{V^p_{n+1}}{\kappa + V^p_{n+1}} - \mu\right)S^p_{n+1} + \omega R^p_{n+1}\right] \\
&\quad + \frac{h^\alpha}{\Gamma(\alpha+2)}\sum_{i=0}^{n} x_{i,n+1}\left[\Lambda\left(\beta_1\frac{I_i + \eta_1 A_i + \eta_2 H_i}{N_i} + \beta_2\frac{I_{ri}}{N_{ri}} + \beta_3\frac{V_i}{\kappa + V_i} - \mu\right)S_i + \omega R_i\right], \\
E_{n+1} &= E_0 + \frac{h^\alpha}{\Gamma(\alpha+2)}\left[\left(\beta_1\frac{I^p_{n+1} + \eta_1 A^p_{n+1} + \eta_2 H^p_{n+1}}{N^p_{n+1}} + \beta_2\frac{I^p_{r_{n+1}}}{N^p_{r_{n+1}}} + \beta_3\frac{V^p_{n+1}}{\kappa + V^p_{n+1}}\right)S^p_{n+1} - (\varepsilon+\mu)E^p_{n+1}\right] \\
&\quad + \frac{h^\alpha}{\Gamma(\alpha+2)}\sum_{i=0}^{n} x_{i,n+1}\left[\left(\beta_1\frac{I_i + \eta_1 A_i + \eta_2 H_i}{N_i} + \beta_2\frac{I_{ri}}{N_{ri}} + \beta_3\frac{V_i}{\kappa + V_i}\right)S_i - (\mu+\varepsilon)E_i\right], \\
A_{n+1} &= A_0 + \frac{h^\alpha}{\Gamma(\alpha+2)}\left(\varepsilon(1-\rho)E^p_{n+1} - \phi_1 A^p_{n+1} - \mu A^p_{n+1}\right) \\
&\quad + \frac{h^\alpha}{\Gamma(\alpha+2)}\sum_{i=0}^{n} x_{i,n+1}\left(\varepsilon(1-\rho)E_i - \phi_1 A_i - \mu A_i\right), \\
I_{n+1} &= I_0 + \frac{h^\alpha}{\Gamma(\alpha+2)}\left(\varepsilon\rho E^p_{n+1} - \phi_3 I^p_{n+1} - \gamma I^p_{n+1} - \delta I^p_{n+1} - \mu I^p_{n+1}\right) \\
&\quad + \frac{h^\alpha}{\Gamma(\alpha+2)}\sum_{i=0}^{n} x_{i,n+1}\left(\varepsilon\rho E_i - \phi_3 I_i - \gamma I_i - \delta I_i - \mu I_i\right), \\
H_{n+1} &= H_0 + \frac{h^\alpha}{\Gamma(\alpha+2)}\left(\gamma I^p_{n+1} - \phi_2 H^p_{n+1} - \delta H^p_{n+1} - \mu H^p_{n+1}\right) \\
&\quad + \frac{h^\alpha}{\Gamma(\alpha+2)}\sum_{i=0}^{n} x_{i,n+1}\left(\gamma I_i - \phi_2 H_i - \delta H_i - \mu H_i\right), \\
R_{n+1} &= R_0 + \frac{h^\alpha}{\Gamma(\alpha+2)}\left(\phi_1 A^p_{n+1} + \phi_2 H^p_{n+1} + \phi_3 I^p_{n+1} - \omega R^p_{n+1} - \mu R^p_{n+1}\right) \\
&\quad + \frac{h^\alpha}{\Gamma(\alpha+2)}\sum_{i=0}^{n} x_{i,n+1}\left(\phi_1 A_i + \phi_2 H_i + \phi_3 I_i - \omega R_i - \mu R_i\right), \\
V_{n+1} &= V_0 + \frac{h^\alpha}{\Gamma(\alpha+2)}\left(\sigma_1 A^p_{n+1} + \sigma_2 H^p_{n+1} + \sigma_3 I^p_{n+1} + \xi I^p_{v_{n+1}} - \nu V^p_{n+1}\right) \\
&\quad + \frac{h^\alpha}{\Gamma(\alpha+2)}\sum_{i=0}^{n} x_{i,n+1}\left(\sigma_1 A_i + \sigma_2 H_i + \sigma_3 I_i + \xi I_{v_i} - \nu V_i\right),
\end{aligned}
$$

$$
\begin{aligned}
S_{r_{n+1}} &= S_{r_0} + \frac{h^\alpha}{\Gamma(\alpha+2)}\left[\Pi - \left(\beta_4 \frac{I^{\,p}_{r_{n+1}}}{N^p_{r_{n+1}}} + \beta_5 \frac{V^p_{n+1}}{\kappa + V^p_{n+1}}\right) S^{\,p}_{v_{n+1}} - \varphi S^{\,p}_{v_{n+1}}\right] \\
&\quad + \frac{h^\alpha}{\Gamma(\alpha+2)} \sum_{i=0}^{n} x_{i,n+1}\left[\Pi - \left(\beta_4 \frac{I_{ri}}{N_{ri}} + \beta_5 \frac{V_i}{\kappa + V_i}\right) S_{r_i} - \varphi S_{r_i}\right], \\
I_{r_{n+1}} &= I_{r_0} + \frac{h^\alpha}{\Gamma(\alpha+2)}\left[\left(\beta_4 \frac{I^{\,p}_{r_{n+1}}}{N^p_{r_{n+1}}} + \beta_5 \frac{V^p_{n+1}}{\kappa + V^p_{n+1}}\right) S^{\,p}_{v_{n+1}} - \varphi I^p_{r_{n+1}}\right] \\
&\quad + \frac{h^\alpha}{\Gamma(\alpha+2)} \sum_{i=0}^{n} x_{i,n+1}\left[\left(\beta_4 \frac{I_{ri}}{N_{ri}} + \beta_5 \frac{V_i}{\kappa + V_i}\right) S_{r_i} - \varphi I_{r_i}\right].
\end{aligned}
$$

where

$$
\begin{aligned}
S^{\,p}_{n+1} &= S_0 + \frac{1}{\Gamma(\alpha)} \sum_{i=0}^{n} y_{i,n+1}\left[\Lambda - \left(\beta_1 \frac{I_i + \eta_1 A_i + \eta_2 H_i}{N_i} + \beta_2 \frac{I_{r_i}}{N_{r_i}} + \beta_3 \frac{V_i}{\kappa + V_i}\right) S_i - \mu S_i + \omega R_i\right], \\
E^p_{n+1} &= E_0 + \frac{1}{\Gamma(\alpha)} \sum_{i=0}^{n} y_{i,n+1}\left[\left(\beta_1 \frac{I_i + \eta_1 A_i + \eta_2 H_i}{N_i} + \beta_2 \frac{I_{ri}}{N_{ri}} + \beta_3 \frac{V_i}{\kappa + V_i}\right) S_i - (\mu + \varepsilon) E_i\right], \\
A^p_{n+1} &= A_0 + \frac{1}{\Gamma(\alpha)} \sum_{i=0}^{n} y_{i,n+1}\left(\varepsilon(1-\rho) E_i - \phi_1 A_i - \mu A_i\right), \\
I^p_{n+1} &= I_0 + \frac{1}{\Gamma(\alpha)} \sum_{i=0}^{n} y_{i,n+1}\left(\varepsilon\rho E_i - \phi_3 I_i - \gamma I_i - \delta I_i - \mu I_i\right), \\
H^p_{n+1} &= H_0 + \frac{1}{\Gamma(\alpha)} \sum_{i=0}^{n} y_{i,n+1}\left(\gamma I_i - \phi_2 H_i - \delta H_i - \mu H_i\right), \\
R^p_{n+1} &= R_0 + \frac{1}{\Gamma(\alpha)} \sum_{i=0}^{n} y_{i,n+1}\left(\phi_1 A_i + \phi_2 H_i + \phi_3 I_i - \omega R_i - \mu R_i\right), \\
V^p_{n+1} &= V_0 + \frac{1}{\Gamma(\alpha)} \sum_{i=0}^{n} y_{i,n+1}\left(\sigma_1 A_i + \sigma_2 H_i + \sigma_3 I_i + \xi I_{v_i} - \nu V_i\right), \\
S^{\,p}_{r_{n+1}} &= S_{r_0} + \frac{1}{\Gamma(\alpha)} \sum_{i=0}^{n} y_{i,n+1}\left[\Pi - \left(\beta_4 \frac{I_{r_i}}{N_{r_i}} + \beta_5 \frac{V_i}{\kappa + V_i}\right) S_{r_i} - \varphi S_{r_i}\right] \\
I^p_{r_{n+1}} &= I_{r_0} + \frac{1}{\Gamma(\alpha)} \sum_{i=0}^{n} y_{i,n+1}\left[\left(\beta_4 \frac{I_{ri}}{N_{r_i}} + \beta_5 \frac{V_i}{\kappa + V_i}\right) S_{r_i} - \varphi I_{r_i}\right].
\end{aligned}
$$

are the predictor values, with

$$
x_{i,n+1} = \begin{cases} n^{\alpha+1} - (n-\alpha)(n+1), & \text{if } i = 0, \\ (n-i+2)^{\alpha+1} + (n-i)^{\alpha+1} - 2(n-i+1)^{\alpha+1} & \text{if } 1 \le i \le n, \\ 1 \quad \text{if } i = n+1, \end{cases}
$$

and

$$
y_{i,n+1} = \frac{h^\alpha}{\alpha}\left((n-i+1)^\alpha - (n-i)^\alpha\right), \quad 0 \le i \le n,
$$

where p is the order of accuracy $p = \min(2, 1+\alpha)$ [48].

3.1. Data fitting and parameter estimation

In this section, Nigerian Lassa fever weekly reported cumulative cases data (from January 03, 2021 to May 19, 2021) is used to fit the model to data and estimate some of the unknown parameters. This improves the acceptance of the model for use in future predictions and to better understand the disease dynamics. The least-squares fit method is used here given its efficiency and reliability. The human natural death rate is estimated as $\mu = \frac{1}{(54.68\times365)}$ per day, where 54.68 years is the average life expectancy in Nigeria, and the estimated total population of Nigeria was 201 million in 2019 [49]. All baseline parameter values obtained from the best fit of the model to cumulative cases data are summarized in Table 3. For the estimated baseline parameter values given in Table 3, we obtained a basic reproduction number, $\mathcal{R}_0 \approx 1.1299$. Figure 2 shows the plot of the reported cumulative confirmed cases data together with the model fit.

Table 3. Description of the model variables.

Parameters	Range	Value	Unit	Source
Λ	–	$\mu \times N_0$	$persons\ day^{-1}$	Estimated
Π	–	10	$mastomys\ rats\ day^{-1}$	Estimated
η_1	(0.5 – 1.0)	0.8512	-	Fitted
η_1	(0.45 – 0.65)	0.5463	-	Fitted
β_1	(0.02 – 0.45)	0.0638	day^{-1}	Fitted
β_2	(0.02 – 0.45)	0.0384	day^{-1}	Fitted
β_3	(0.02 – 0.552)	0.0200	day^{-1}	Fitted
β_4	(0.02 – 0.552)	0.0913	day^{-1}	Fitted
κ	(1000 – 10000)	9787.3	$virus$	Fitted
ω	(0.003 – 0.005)	0.0034	day^{-1}	Fitted
ε	(0.2 – 0.5)	0.2011	day^{-1}	Fitted
ρ	(0.1 – 1.0)	0.2383	-	Fitted
ϕ_1	(0.045 – 0.09)	0.0494	day^{-1}	Fitted
ϕ_2	(0.045 – 0.09)	0.0715	day^{-1}	Fitted
ϕ_3	(0.045 – 0.09)	0.0510	day^{-1}	Fitted
γ	(0.05 – 0.9)	0.4832	day^{-1}	Fitted
δ	(0.15 – 0.35)	0.1662	day^{-1}	Fitted
σ_1	(0.25 – 0.35)	0.3004	day^{-1}	Fitted
σ_2	(0.2 – 0.3)	0.2331	day^{-1}	Fitted
σ_3	(0.3 – 0.45)	0.4379	day^{-1}	Fitted
ξ	(0.4 – 0.55)	0.4136	day^{-1}	Fitted
ν	(0.3 – 0.55)	0.4353	day^{-1}	Fitted
β_5	(0.02 – 0.552)	0.1212	day^{-1}	Fitted
ψ	–	0.0020	day^{-1}	[50]

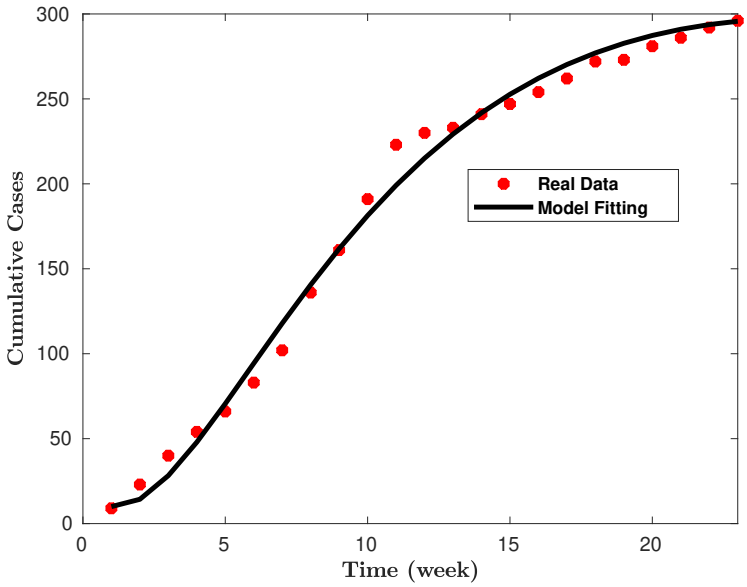

Figure 2. Model fitting with confirmed cases in Nigeria.

3.2. Sensitivity analysis

To examine the effect of parameter changes on $\mathcal{R}_0$, we used Latin Hypercube Sampling (LHS) [51–53] and computed the partial rank correlation coefficients (PRCCs) of the sampled input model parameters with corresponding value of the basic reproduction number $\mathcal{R}_0$ as the output. To determine which parameters are significant, p-values of corresponding PRCCs are calculated for the respective parameters after Fisher transformation [51, 52]. The calculated PRCCs for the sampled input parameters and their corresponding p-values are given in Table 4.

Table 4. Parameter PRCC Significance (Unadjusted p-values).

Parameter	PRCC	p-value	Keep
η_1	0.0268	4.004×10^{-1}	False
η_2	0.0190	5.511×10^{-1}	False
β_1	0.0426	1.812×10^{-1}	False
β_2	0.0820	9.937×10^{-3}	True
β_3	0.7775	0.000	True
ε	-0.0194	5.428×10^{-1}	False
ρ	-0.5210	0.000	True
γ	-0.0131	6.811×10^{-1}	False
σ_1	0.1105	5.006×10^{-4}	True
σ_2	0.0307	3.354×10^{-1}	False
σ_3	0.0001	9.975×10^{-1}	False
ξ	-0.0012	9.700×10^{-1}	False
ν	-0.2579	2.220×10^{-16}	True
φ	-0.0681	3.239×10^{-2}	True

Figure 3(a) gives the summary of calculated PRCCs in the tornado plot, and the basic reproduction number values ($\mathcal{R}_0$) computed (minimum value, lower quartile, median, upper quartile, and maximum value) are summarized in the boxplot, Figure 3(b). In Figure 3(b), it is clear that there are outliers. The major interest in containing the disease is to find combinations of processes that can reduce the value of $\mathcal{R}_0$ below 1. Despite the fact that the median value for $\mathcal{R}_0$ is close to 1, there may be a variety of combinations of processes that can worsen the epidemic. We note that the process described by the parameter β_3 with the highest positive PRCCs has the highest potential of worsening disease when it increases. We note that improving hygiene, reduces the pontential of contracting the virus from potentially infected surfaces. Therefore, it is recommended that improving hygiene practices is essential in overcoming the disease burden. On the other hand, the parameters (ν and ρ) with the highest negative PRCCs have the greatest potential to contain the infection when maximized. In this respect, we further note that increasing the pathogen decay rate by disinfecting surfaces, practicing good hygiene, reducing the shedding of the virus into the environment, and earlier diagnostics to identify people with asymptomatic infections are key in effectively curtailing the infection.

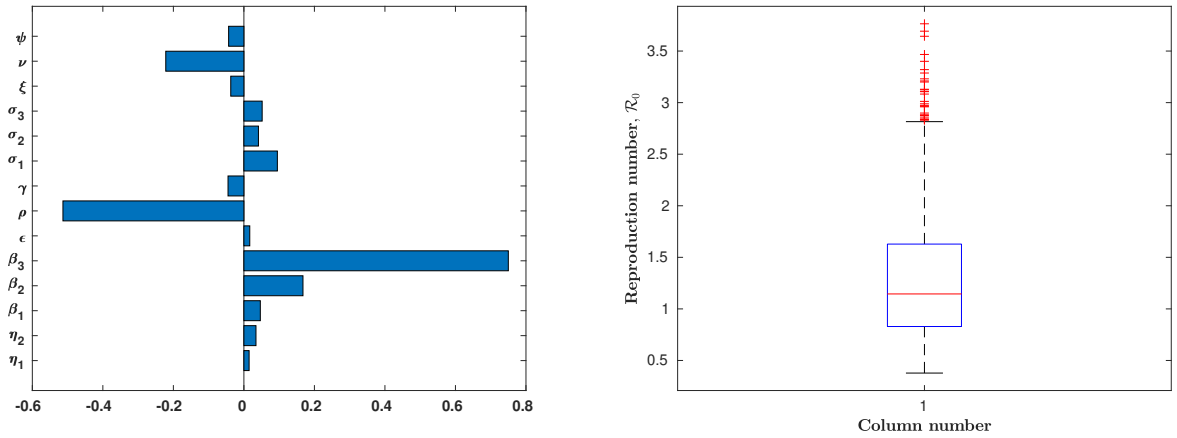

(a) **(b)**

Figure 3. Partial rank correlation coefficients (PRCCs) of sampled parameter values. (a) shows a tornado plot summarising the PRCCs from sampled parameters, where positive PRCCs indicate a process that can worsen the epidemic if the epidemic progresses, and those with negative PRCCs can help control the disease, (b) The box plot displays the $\mathcal{R}_0$ values calculated from the sampling procedure (that is, minimum, lower quartile, median, upper quartile, and maximum values).

The values of input parameters with significant PRCCs (p-values less than 0.05) are compared pairwise to determine if the processes described by these parameters are significantly different. The null hypothesis, H_0, is that there are significant differences between the compared parameters [52]. To minimise the likelihood of making a Type I statistical error, False discovery rate (FDR) adjusment is performed during the comparison. The summary of p-values from the comparisons is given in Table 5. The results in Table 5 are summarized in Table 6, where "True" indicates significant differences between the compared parameters, while "False" indicates otherwise.

Table 5. Pairwise PRCC Comparisons (FDR Adjusted p-values).

	β_2	β_3	ρ	σ_1	ν	φ
β_2		0	0	0.5234	2.464×10^{-14}	0.0009112
β_3			0	0	0	0
ρ				0	4.587×10^{-12}	0
σ_1					0	8.158×10^{-5}
ν						1.782×10^{-5}
φ						

Table 6. *Parameters different after FDR adjustment?*

	β_2	β_3	ρ	σ_1	ν	φ
β_2		True	True	False	True	True
β_3			True	True	True	True
ρ				True	True	True
σ_1					True	True
ν						True
φ						

3.3. Results and discussion

In this section, we present the numerical results of the model simulations obtained for different scenarios. From Figure 4, the results show that the infected populations are characterized by an initial rapid increase, reaching maximum values, and then a decline to a relative equilibrium. The initial rapid increase is due to availability of a high number of susceptible individuals who can be infected and thus is associated with high infection probability. The subsequent decline in the number of infections is due to the disease's self-limitation, which results from a decrease in contacts owing to a low number of susceptible individuals. In addition, decreasing the number of susceptible or infected hosts or vectors reduces the possibility of contact, thereby reducing the likelihood of new infections. For the fractional-order considerations, when the order of the derivative (α) decreases, the epidemiological system is characterized by an increase in the memory effect (high dependence of future on the previous states), resulting in a slow growth but high long-term equilibrium numbers compared to the integer-order case. Compared to the integer-order case, the results from the fractional-order model predict lower epidemic peaks. However, the disease is predicted to remain highly prevalent in the population for a long period of time.

To observe the effects of human-to-human transmission contact rate on the number of infections, we simulate the model using different parameter values of β_1, with the baseline value being the numerical value obtained from the model fitting. The reduction in human-to-human transmission rate can lead to a drop in the number of infected cases, as seen in Figure 5. For instance, decreasing β_1 by 25% and 50%, reduces the infection peak values from 33 to 31 and 29 respectively, leaving the disease at its endemic state as shown in Figure 5(a). As a result, the disease burden can be kept at minimal values by decreasing the rate of infection transfer from person to person. To minimize person-to-person transmission, someone needs to take preventive precautions against contact with patients' secretions,

especially in a hospital setting. We note that wearing protective clothes such as masks, gloves, protective gowns and goggles, using infection control methods such as full equipment sterilization, and isolating sick patients from contact with potentially susceptible persons are all examples of preventative measures. Capturing and grooming or using mastomy rats as a food source may lead to an increase disease transmission. Minimizing the rat-to-human transmission rate, reduces the number of infections as shown in Figure 6. Furthermore, one factor that aids in the transmission of the disease is the environmental contamination with Lassa virus. Disinfecting the environment and imposing strict sanitation measeures to reduce the effective contact rate of the population with the contaminated environment may help curb new infections. Morestill, storage of food in mastomys rat-proof containers, and keeping the homes clean, helps to discourage rodents from entering homes. In addition, disposing off garbage far from the home can help sustain clean households. The effect of decreasing environmental control mechanisms is simulated and the results are presented in Figure 7. In particular, Figure 7(a) shows that the value of the baseline parameter $\beta_3 = 0.0482$, draws the corresponding infection peak closer to 33. We note that, decreasing the value of β_3 by 50% reduces the human infection peak to 30. In cases where the affected population is in thousands, this change will definitely be very significant and can overwhelm the healthcare system. The infection trend observed with increased memory (when α =0.8), see Figure 7(b) is associated with higher longterm numbers of infected individuals.

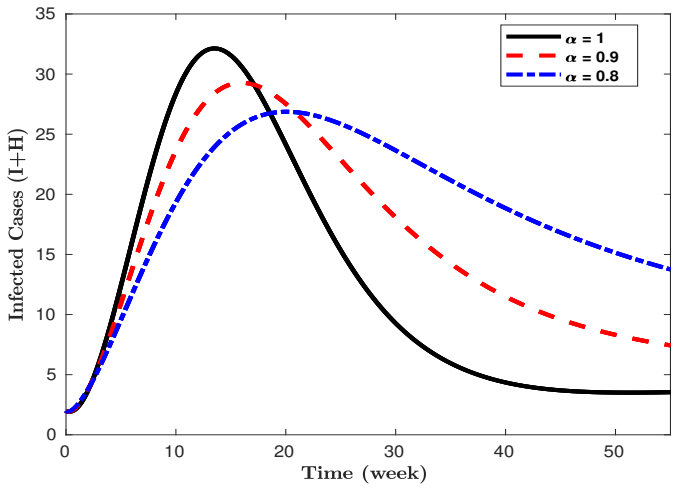

Figure 4. Model simulation of the disease dynamics depicting weekly new cases when $\alpha = 1, 0.9, 0.8$.

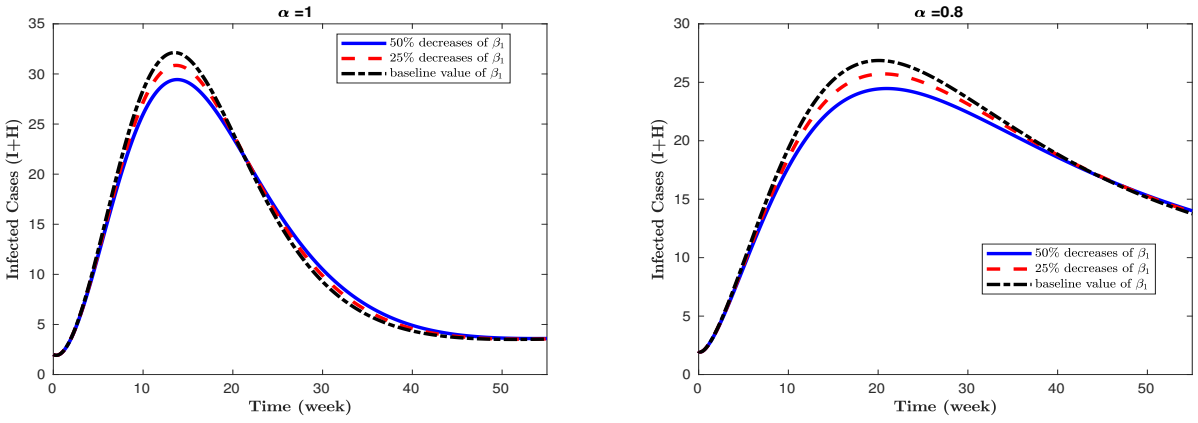

(a) **(b)**

Figure 5. Impact of person-to-person contact probability, β_1 on the number of new infections when (a) $\alpha = 1.0$, and (b) $\alpha = 0.8$

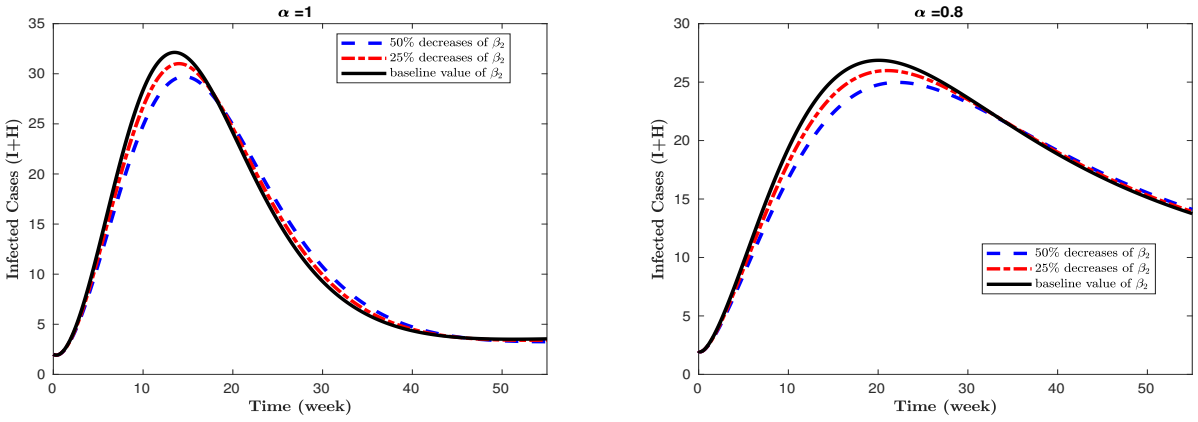

(a) **(b)**

Figure 6. Impact of mastomy rat to human contact probability, β_2 on the number of new infections when (a) $\alpha = 1.0$, and (b) $\alpha = 0.8$.

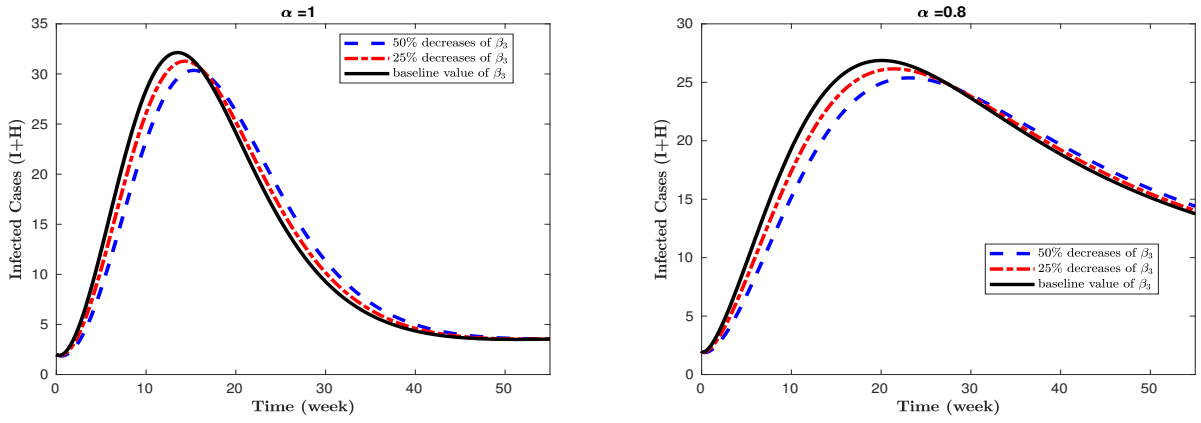

(a) **(b)**

Figure 7. Impact of environmental contaminated transmission probability, β_3 on the number of new infections when (a) $\alpha = 1.0$, and (b) $\alpha = 0.8$.

4. Conclusions

In this work, a fractional-order model for Lassa fever transmission dynamics is presented. The model incorporates person-to-person contacts, mastomys rat-to-human transmission as well as transmission from a contaminated environment. To guarantee that the model is well-posed, basic characteristics such as non-negativity of solutions given non-negative initial values, and boundedness of solutions were proved. The disease-free equilibrium and its stability as well as the model basic reproduction number were determined. To estimate the model parameter values, the model was fitted to Nigeria's Lassa fever weekly reported cumulative cases for the period January 03, 2021 to May 19, 2021. For the estimated baseline parameter values from the data fit, we obtained a basic reproduction number, $\mathcal{R}_0 \approx 1.1299$. Sensitivity analysis using the LHS was carried to determine the parameters which describe the processes that are more significant in reducing the reproduction number and consequently curtailing the disease. From sensitivity analysis results, the rate of human contact with contaminated surfaces, and the decay of the virus from the environment were observed to be of significant influence. Consequently, the processes described by such parameters have the greatest potential of curtailing Lassa fever. Our overall results recommend various interventions and control measures which include; controlling environmental transmission, rodents-to-humans transmission, and humans-to-humans transmission. These intervention measures have a great pontential for containing Lassa fever in the community. In addition, environmental control and disinfecting surfaces are associated with lower and delayed peaks of infections. It is also strongly recommended that all suspected Lassa fever infections be diagnosed early to identify people with asymptomatic infections. We noted that when dependence of future values on previous states increases (ie. as α reduces from 1 toward 0) the infection slows down and reaches a peak lower than that reached by a system with a higher order of the fractional derivative. On the other hand, in long-term dynamics, equilibrium cases are inversely proportional to the order of the fractional derivative of the system. That is, a slow rate of infection growth in the system with lower orders of the fractional derivatives is characterized by infected cases peaks occuring at a later time when compared to the system with a higher fractional

order. Moreover, we observed that taking prescribed self-protection measures for large numbers of people who have known similar infections in the past can slow down a potentially explosive outbreak. Therefore, the study can be extended further to include the effect of disease awareness for a better understanding of the disease and extensive implementation of control strategies. Additionally, this work can be extended by using the stochastic forecasting approach detailed in [54]. Lastly, the results of the study can provide guidance to local disease control programs when planning and designing cost-effective strategies for eliminating the disease from Nigeria and West Africa as a whole.

Acknowledgments

J. P. Ndenda gratefully acknowledges the funding received from the Simons Foundation (US) through The Research and Graduate Studies in Mathematics (RGSMA) project at Botswana International University of Science and Technology (BIUST) and the Research Initiation Grant (Project number S00212 at BIUST).

Conflict of interest

The authors declare no conflict of interest.

References

1. Lassa fever. Available from: `https://www.ncdc.gov.ng/diseases/factsheet/47`.
2. Lassa fever. Available from: `https://www.cdc.gov/vhf/lassa/index.html`.
3. Lassa fever. Available from: `https://www.who.int/health-topics/lassa-fever`.
4. K. M. Johnson, T. P. Monath, Imported Lassa fever-reexamining the algorithms, Technical report, Army Medical Research Inst of Infectious diseases Fort Detrick MD, 1990.
5. M. S. Mahdy, W. Chiang, B. McLaughlin, K. Derksen, B. H. Truxton, K. Neg, Lassa fever: the first confirmed case imported into Canada, *Canada diseases weekly report = Rapport hebdomadaire des maladies au Canada*, **15** (1989), 193–198.
6. R. M. Zweighaft, D. W. Fraser, M. A. W. Hattwick, W. G. Winkler, W. C. Jordan, M. Alter, et al., Lassa fever: response to an imported case, *N. Eng. J. Med.,* **297** (1977), 803–807. http://dx.doi.org/10.1056/NEJM197710132971504
7. C. M. Hadi, A. Goba, S. H. Khan, J. Bangura, M. Sankoh, S. Koroma, et al., Ribavirin for Lassa fever postexposure prophylaxis, *Emerg. Infect. Dis.,* **16** (2010), 2009–2011. http://dx.doi.org/10.3201/eid1612.100994
8. A. R. Akhmetzhanov, Y. Asai, H. Nishiura, Quantifying the seasonal drivers of transmission for Lassa fever in Nigeria, *Phil. Trans. R. Soc. B,* **374** (2019), 20180268. https://doi.org/10.1098/rstb.2018.0268
9. I. S. Onah, O. C. Collins, Dynamical system analysis of a Lassa fever model with varying socioeconomic classes, *J. Appl. Math.*, **2020** (2020), 2601706. https://doi.org/10.1155/2020/2601706

10. J. Mariën, B. Borremans, F. Kourouma, J. Baforday, T. Rieger, S. Günther, et al., Evaluation of rodent control to fight Lassa fever based on field data and mathematical modelling, *Emerg. Microbes Infect.,* **8** (2019), 640–649. https://doi.org/10.1080/22221751.2019.1605846

11. E. Fichet-Calvet, D. J. Rogers, Risk maps of Lassa fever in West Africa, *PLOS Negl. Trop. Dis.,* **3** (2009), e388. https://doi.org/10.1371/journal.pntd.0000388

12. S. Dachollom, C. E. Madubueze, Mathematical model of the transmission dynamics of Lassa fever infection with controls, *Math. Model Appl.,*, **5** (2020), 65–86. https://doi.org/10.11648/j.mma.20200502.13

13. M. M. Ojo, B. Gbadamosi, T. O. Benson, O. Adebimpe, A. L Georgina, Modeling the dynamics of Lassa fever in Nigeria, *J. Egypt Math. Soc.,* **29** (2021), 1–19. https://doi.org/10.1186/s42787-021-00124-9

14. H. Khan, J. F. Gómez-Aguilar, A. Alkhazzan, A. Khan, A fractional order HIV-TB coinfection model with nonsingular Mittag-Leffler Law, *Math. Methods Appl. Sci.,* **43** (2020), 3786–3806. https://doi.org/10.1002/mma.6155

15. S. Patnaik, F. Semperlotti, Application of variable-and distributed-order fractional operators to the dynamic analysis of nonlinear oscillators, *Nonlinear Dyn.*, **100** (2020), 561–580. https://doi.org/10.1007/s11071-020-05488-8

16. J. P. Ndenda, J. B. H. Njagarah, S. Shaw, Role of immunotherapy in tumor-immune interaction: Perspectives from fractional-order modelling and sensitivity analysis, *Chaos Soliton. Fract.,* **148** (2021), 111036. https://doi.org/10.1016/j.chaos.2021.111036

17. M. Onal, A. Esen, A Crank-Nicolson approximation for the time fractional Burgers equation, *Appl. Math. Nonlinear Sci.*, **5** (2020), 177–184. https://doi.org/10.2478/amns.2020.2.00023

18. J. P. Ndenda, J. B. H. Njagarah, C. B. Tabi, Fractional-Order model for myxomatosis transmission dynamics: Significance of contact, vector control and culling, *SIAM J. Appl. Math.,* **81** (2021), 641–665. https://doi.org/10.1137/20M1359122

19. J. B. H. Njagarah, C. B. Tabi, Spatial synchrony in fractional order metapopulation cholera transmission, *Chaos Soliton. Fract.,* **117** (2018), 37–49. https://doi.org/10.1016/j.chaos.2018.10.004

20. A. K. Singh, M. Mehra, S. Gulyani, A modified variable-order fractional SIR model to predict the spread of COVID-19 in India, *Math. Meth. Appl. Sci.*, **2021** (2021), 1–15. https://doi.org/10.1002/mma.7655

21. A. Aghili, Complete solution for the time fractional diffusion problem with mixed boundary conditions by operational method, *Appl. math. nonlinear sci.,* **6** (2020), 9–20. https://doi.org/10.2478/amns.2020.2.00002

22. I. Podlubny, *Fractional differential equations: an introduction to fractional derivatives, fractional differential equations, to methods of their solution and some of their applications*, Volume 198, 1st Ed., Elsevier, 1998.

23. A. A. Kilbas, H. M. Srivastava, J. J. Trujillo, *Theory and applications of fractional differential equations*, volume 204, 1st Ed., Elsevier, 2006.

24. D. Kaur, P. Agarwal, M. Rakshit, M. Chand, Fractional calculus involving (p,q)-mathieu type series, *Appl. Math. Nonlinear Sci.,* **5** (2020), 15–34. https://doi.org/10.2478/amns.2020.2.00011

25. K. A. Touchent, Z. Hammouch, T. Mekkaoui, A modified invariant subspace method for solving partial differential equations with non-singular kernel fractional derivatives, *Appl. Math. Nonlinear Sci.,* **5** (2020), 35–48. https://doi.org/10.2478/amns.2020.2.00012

26. A. O. Akdemir, E. Deniz, E. Yüksel, On some integral inequalities via conformable fractional integrals, *Appl. Math. Nonlinear Sci.,* **6** (2021), 489–498. https://doi.org/10.2478/amns.2020.2.00071

27. M. Gürbüz, E. Yldz, Some new inequalities for convex functions via Riemann-Liouville fractional integrals, *Appl. Math. Nonlinear Sci.,* **6** (2021), 537–544. https://doi.org/10.2478/amns.2020.2.00015

28. H. M. Srivastava, Some parametric and argument variations of the operators of fractional calculus and related special functions and integral transformations, *J. Nonlinear Convex Anal,*, **22** (2021), 1501–1520.

29. H. M. Srivastava, An introductory overview of fractional-calculus operators based upon the Fox-Wright and related higher transcendental functions, *J. Adv. Eng. Comput.*, **5** (2021), 135–166. http://dx.doi.org/10.25073/jaec.202153.340

30. M. Caputo, M. Fabrizio, A new definition of fractional derivative without singular kernel, *Progr. Fract. Differ. Appl.,* **1** (2015), 73–85. https://dx.doi.org/10.12785/pfda/010201

31. A. Atangana, J. F. Gómez-Aguilar, Numerical approximation of Riemann-Liouville definition of fractional derivative: from Riemann-Liouville to Atangana-Baleanu. *Numer. Methods Partial Differ. Equ.,* **34** (2018), 1502–1523. https://doi.org/10.1002/num.22195

32. N. Gul, R. Bilal, E. A. Algehyne, M. G. Alshehri, M. A. Khan, Y. Chu, et al., The dynamics of fractional order Hepatitis B virus model with asymptomatic carriers, *Alex. Eng. J.,* **60** (2021), 3945–3955. https://doi.org/10.1016/j.aej.2021.02.057

33. J. F. Gomez-Aguilar, T. Cordova-Fraga, T. Abdeljawad, A. Khan, H. Khan, Analysis of fractal-fractional malaria transmission model, *Fractals,* **28** (2020), 2040041. https://doi.org/10.1142/S0218348X20400411

34. E. Uçar, N. Özdemir, A fractional model of cancer-immune system with Caputo and Caputo-Fabrizio derivatives, *Eur. Phys. J. Plus*, **136** (2021), 1–17. https://doi.org/10.1140/epjp/s13360-020-00966-9

35. B. Ghanbari, On the modeling of the interaction between tumor growth and the immune system using some new fractional and fractional-fractal operators, *Adv. Differ. Equ.,*. **2020** (2020), 585. https://doi.org/10.1186/s13662-020-03040-x

36. S. T. M. Thabet, M. S. Abdo, K. Shah, Theoretical and numerical analysis for transmission dynamics of COVID-19 mathematical model involving Caputo-Fabrizio derivative, *Adv. Differ. Equ.,* **185** (2021), 1–17. https://doi.org/10.1186/s13662-021-03316-w

37. S. Rezapour, H. Mohammadi, M. E. Samei, SEIR epidemic model for COVID-19 transmission by Caputo derivative of fractional order, *Adv. Differ. Equ.,* **490** (2020), 1–19. https://doi.org/10.1186/s13662-020-02952-y

38. D. Baleanu, H. Mohammadi, S. Rezapour, A fractional differential equation model for the COVID-19 transmission by using the Caputo-Fabrizio derivative, *Adv Differ Equ.,* **299** (2020), 1–27. https://doi.org/10.1186/s13662-020-02762-2

39. P. A. Naik, M. Yavuz, S. Qureshi, J. Zu, S. Townley, Modeling and analysis of COVID-19 epidemics with treatment in fractional derivatives using real data from Pakistan, *Eur. Phys. J. Plus,* **135** (2020), 1–42. https://doi.org/10.1140/epjp/s13360-020-00819-5

40. M. ur Rahman, S. Ahmad, R. T. Matoog, N. A. Alshehri, T. Khan, Study on the mathematical modelling of COVID-19 with Caputo-Fabrizio operator, *Chaos Soliton. Fract.,* **150** (2021), 111121. https://doi.org/10.1016/j.chaos.2021.111121

41. T. A. Biala, A. Q. M. Khaliq, A fractional-order compartmental model for the spread of the COVID-19 pandemic, *Commun. Nonlinear. Sci. Numer. Simul.,* **98** (2021), 105764. https://doi.org/10.1016/j.cnsns.2021.105764

42. H. Singh, H. M. Srivastava, Z. Hammouch, K. S. Nisar, Numerical simulation and stability analysis for the fractional-order dynamics of COVID-19, *Results Phys.*, **20** (2021), 103722. https://doi.org/10.1016/j.rinp.2020.103722

43. R. Gorenflo, A. A. Kilbas, F. Mainardi, S. V. Rogosin, *Mittag-Leffler functions, related topics and applications*, volume 2, Springer, 2014.

44. S. Choi, B. Kang, N. Koo, Stability for Caputo fractional differential systems, *Abstr. Appl. Anal.*, **2014** (2014), 631419. https://doi.org/10.1155/2014/631419

45. P. Van den Driessche, J. Watmough, Reproduction numbers and sub-threshold endemic equilibria for compartmental models of disease transmission, *Math. Biosci.,* **180** (2002), 29–48. https://doi.org/10.1016/S0025-5564(02)00108-6

46. J. Losada, J. J. Nieto, Properties of a new fractional derivative without singular kernel, *Progr. Fract. Differ. Appl.,* **1** (2015), 87–92. https://dx.doi.org/10.12785/pfda/010202

47. K. Diethelm, N. J. Ford, A. D. Freed, A predictor-corrector approach for the numerical solution of fractional differential equations, *Nonlinear Dynam.*, **29** (2002), 3–22. https://doi.org/10.1023/A:1016592219341

48. K. Diethelm, N. J. Ford, A. D. Freed, Detailed error analysis for a fractional Adams method, *Numer. Algorithms*, **36** (2004), 31–52. https://doi.org/10.1023/B:NUMA.0000027736.85078.be

49. *Population of Nigeria*, Available from: `https://data.worldbank.org/country/nigeria`.

50. S. S. Musa, S. Zhao, D. Gao, Q. Lin, G. Chowell, D. He, Mechanistic modelling of the large-scale Lassa fever epidemics in Nigeria from 2016 to 2019, *J. Theor. Biol.,* **493** (2020), 110209. https://doi.org/10.1016/j.jtbi.2020.110209

51. S. M. Blower, H. Dowlatabadi, Sensitivity and uncertainty analysis of complex models of disease transmission: An HIV model, as an example, *Int. Stat. Rev. /Revue Internationale de Statistique*, **62** (1994), 229–243. https://doi.org/10.2307/1403510

52. S. M Kassa, J. B. H Njagarah, Y. A Terefe, Analysis of the mitigation strategies for COVID-19: From mathematical modelling perspective, *Chaos Soliton. Fract.*, **138** (2020), 109968. https://doi.org/10.1016/j.chaos.2020.109968

53. F. Nyabadza, J. B. H. Njagarah, R. J. Smith, Modelling the dynamics of crystal meth ('tik') abuse in the presence of drug-supply chains in South Africa, *B. Math. Biol.*, **75** (2013), 24–48. https://doi.org/10.1007/s11538-012-9790-5

54. H. Singh, H. M. Srivastava, Z. Hammouch, K. S. Nisar, Mathematical modeling approach to predict COVID-19 infected people in Sri Lanka, *AIMS Math.*, **7** (2022), 4672–4699. https://doi.org/10.3934/math.2022260

AIMS Press

© 2022 the Author(s), licensee AIMS Press. This is an open access article distributed under the terms of the Creative Commons Attribution License (http://creativecommons.org/licenses/by/4.0)